Application note

Band Gap Analysis through UV-Visible Spectroscopy

Introductions

Semiconducting materials are often analyzed using UV-Visible spectroscopy to learn more about the electronic structure of the substances.[1-3] For semiconductors, the electronic structure is not defined in the same manner that small molecules are described. In these materials, the electronic states are clustered very close in energy to one another, resulting in a band of electronic states instead of discrete energy levels. The highest filled energy band, analogous to the highest occupied molecular orbital (HOMO) for small molecules, is referred to as the valence band (VB); the lowest unoccupied energy band, similar to the lowest unoccupied molecular orbital (LUMO) in molecules, is referred to as the conduction band (CB).[4]

The top of the VB and bottom of the CB in semiconductors are separated by an energy gap, referred to as the band gap (E_g) as shown in Figure 1.[4,5] Unlike metals, where electrons can freely move, this separation in semiconductors prevents the transfer of electrons to the conduction band under standard conditions. Electrons occupying the VB can be promoted to the CB given enough energy is supplied to equal or surpass E_g. This can be accomplished through either applying a potential across the material or through irradiation of the material with the appropriate wavelength of light.

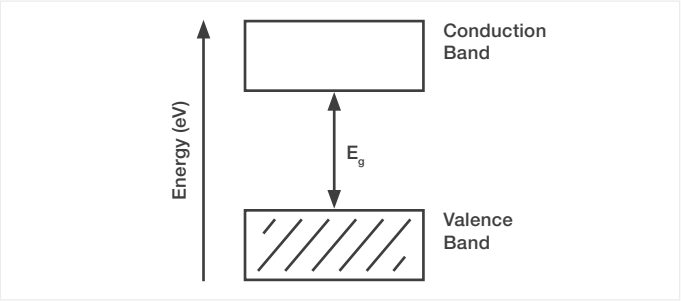

Figure 1. General electronic structure for semiconducting materials. Eg refers to the band gap energy and is typically reported in eV units.

Information about the electronic structure of the material can be important to determine, as this can have ramifications for photo-induced processes within the material like photocatalysis[6] or solar energy conversion.[2] In combination with other methods, such as electrochemical analysis (e.g., cyclic voltammetry),[7] ultraviolet photoelectron spectroscopy (UPS)[8], and computational calculations,[2] this information can be used to understand the position of the CB and VB relative to a standard electrode reference. Because UV-Visible absorption and reflectance spectra arise from transitions between occupied and unoccupied states, these spectral measurements can be directly used to estimate E_g.

Traditionally, the band gap energy is determined through use of a Tauc analysis, by which the band gap energy is related to the absorption coefficient through the following equation,

$$(\alpha h\nu)^{\frac{1}{\gamma}} = B(h\nu - E_g)$$

Equation 1.

where α is the absorption coefficient, h is Plank's constant (6.63×10^{-34} J•s), ν is the frequency of the incident photon, γ is a parameter reflecting the nature of the band gap transition (e.g., direct/indirect, allowed/forbidden), B is the slope of the linear portion of the Tauc Plot and E_g is the band gap energy.[1,9,10] The Tauc plot is constructed by reporting the collected spectrum as $\alpha h\nu^{(1/\gamma)}$ vs. Energy (eV). As absorbance is proportional to α through Beer's law, the collected absorbance can be used in place of the absorption coefficient to develop the curve. The energy axis is determined by converting the analyzed wavelength spectrum to energy through equation 2,

$$E = \frac{hc}{\lambda}$$

Equation 2.

where E is the converted energy, c is the speed of light (3.0×10^8 m/s), h, as before, is Plank's constant and λ is the wavelength of light. By convention, the calculated energy is converted from J to eV. From the curve, a tangent line can be fit to the linear section of the data. The intersection of the tangent line with the x-axis denotes the estimated band gap energy of the material.

If the material can be suspended in a liquid and results in an optically clear, non-turbid solution, then the measured absorbance of the colloidal solution can be used in the Tauc plot analysis.[9] However, for powders and non-transparent solid samples reflectance measurements are the appropriate method for analysis. Due to the irregularity of the surface of particles within the powder or thin films, these reflections are primarily diffuse in nature, implying there are likely fewer specular reflections observed. Diffuse reflections are often directed at multiple different angles, including away from the detector, leading to an unintentional omission of reflections during the experiment.

To avoid this issue, an integrating sphere can be used to collect all light reflected by the material. As implied by its name, the interior of this accessory is spherical and coated with a highly reflective substance. When light diffusively reflects off the sample, the reflections bounce of the interior coating many times until it is directed towards the detector. Without the sphere, these diffuse reflections would not be able to reach the detector and would not be included in the reflectance spectrum. Alternatively, diffuse reflectance accessories, like the Thermo Scientific™ Praying Mantis™ Diffuse Reflectance Accessory, can also be used to collect the diffuse reflections without the use of an integration sphere.

Under circumstances where thin films or powdered semiconducting samples are studied, the diffuse reflectance spectrum can be collected and reported in place of absorbance using the Kubelka-Munk formulism (equation 3),

$$F(R) = \frac{(1-R)^2}{2R}$$

Equation 3.

where *F(R)* is the Kubelka-Munk value (unitless), and *R* is the collected percent reflectance (%R) of the sample as a function of wavelength.[1,10] *F(R)* is directly proportional to the absorption coefficient according to equation 4,

$$F(R) = \frac{k}{s}$$

Equation 4.

where *k* is the absorption coefficient, and *s* is the scattering coefficient.[3,12] Using this transformation in place of α, the Tauc plot can be constructed for powder and film samples, allowing for a determination of E_g.

As an example, the reflectance spectrum of two powdered TiO_2 samples of differing crystal structure (rutile and anatase), both well- characterized semiconducting materials,[11,12] were acquired using the Thermo Scientific™ Evolution™ One Plus UV-Visible Spectrophotometer, equipped with an ISA-220 Integrating Sphere, and an appropriate powder sample holder. Similarly, the same experiment was performed using the Thermo Scientific™ Evolution™ Pro UV-Visible Spectrophotometer and the Praying Mantis diffuse reflectance accessory. Through the collected spectra, Tauc plots were generated and compared between both instruments. The resulting E_g for each respective sample not only match using measurements acquired on different instruments, but also agree with literature, demonstrating the ability to quickly analyze the bandgap energy of solid-state semiconductors through the analysis of UV-Visible spectra.

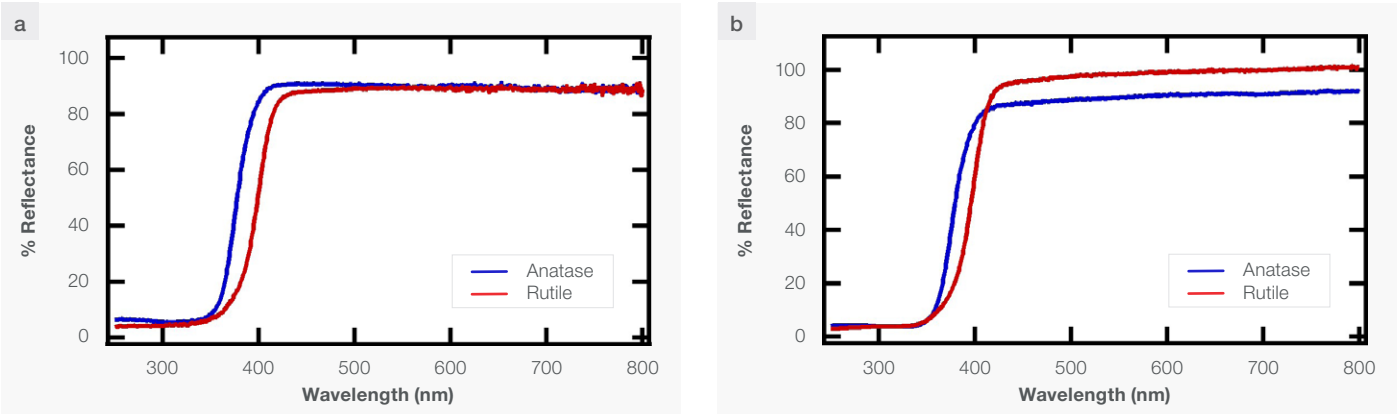

Figure 2. Diffuse reflectance spectra of anatase (blue) and rutile (red) TiO_2. Spectra were collected using (a) the ISA-220 integrating sphere and (b) the Praying Mantis diffuse reflectance accessory.

Experimental

Both anatase and rutile TiO_2 samples were measured as received using the Evolution One Plus equipped with an integrating sphere (ISA-220) and the Evolution Pro with the Praying Mantis. For data collected using the Evolution One Plus and ISA, the sample was held in a powder sample holder and measured without using an 8° wedge, allowing for collection of only diffuse reflections. With both accessories, the %R spectrum was collected between 250 nm and 800 nm using a 1.0 nm bandwidth and 1.0 nm step size. The data was integrated for 0.25 s using the Praying Mantis and for 0.5 s using the ISA-220. The background was collected using a white Spectralon reference material for measurements collected using the ISA-220, while a PTFE diffuse reflectance disk was used for measurements collected using the Praying Mantis.

Results/Discussion

To demonstrate this analysis, the %R spectra of two different TiO_2 nanoparticles of different crystal structure, anatase and rutile, were measured using the Evolution One Plus. As these samples were analyzed in powder form, the ISA-220, an integrating sphere accessory, was used. As can be seen in the reflectance spectra in Figure 2a, both TiO_2 samples do not reflect a substantial amount of UV light below 350 nm, however the onset observed for rutile is at a slightly longer wavelength than for the anatase TiO_2 sample. As the wavelength and energy of a photon is inversely proportional according to equation 2, this implies that the bandgap energy is likely smaller for the rutile TiO_2 sample than for the anatase sample.

For samples with limited amount of material, the Praying Mantis Diffuse Reflectance Accessory can also be used for the same analysis. This accessory allows for the measurement of diffuse reflections of powder substance. These materials can be held in sample holders with a total volume of 250 mm^3 (macro holder) or 31.6 mm^3 (micro holder). Unlike an integrating sphere, this accessory only collects the diffuse reflections from a material. Additionally, this apparatus can be used in tandem with a reaction chamber to provide an inert environment, introduce reaction gases to the powdered sample, or control the temperature of the material. This can be particularly helpful for *in-situ* analysis of the UV-Visible reflectance spectrum of materials used in high-temperature catalytic reactions held at the appropriate temperature.

The same diffuse reflectance measurements were performed using the Evolution Pro and Praying Mantis, as reported in Figure 2b. The data collected shows a similar trend as the measurements acquired using the integrating sphere. A minimal amount of light below 350 nm is reflected for both samples, while the onset for rutile TiO_2 begins at a longer wavelength than the onset for anatase TiO_2. However, at longer wavelengths, the %R recorded for both samples do not appear to perfectly match when comparing measurements collected with the integrating sphere and Praying Mantis accessories.

It is important to note that the %R spectra collected using the integrating sphere or Praying Mantis are relative measurements, not absolute. This is due to the method used to determine the initial intensity of the light prior to interacting with the sample. Because a standard such as Spectralon or PTFE is required to establish the initial light intensity, the %R will be dependent on how well the standard reflects light. As such, measuring samples using different reflectance standards can result in slight variations in overall measured spectrum intensity, especially in regions where most or all of the light is reflected by the sample. Additionally, variations in the Y-axis may arise as a result of variations in the amount of material probed due to differences in the angle of incidence between the two accessories.

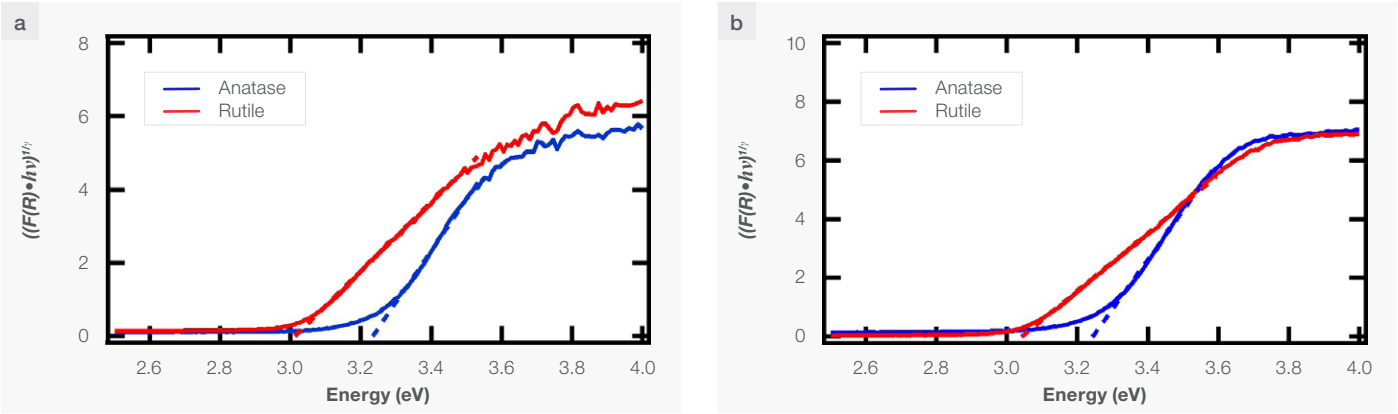

Figure 3. Tauc Plot for rutile (red) and anatase (blue) TiO_2 collected using (a) an integrating sphere and (b) the Praying Mantis diffuse reflectance accessory. The dashed lines are the tangent lines fit to the linear portion of the spectrum. As TiO_2 has an indirect band gap, $\gamma = 2$.

Using the methodology described earlier, Tauc Plots were constructed from the reflectance measurements for these samples (Figure 3). TiO_2 has been extensively studied and has a well-defined indirect band gap for both crystal structures analyzed herein. From the Tauc analysis, E_g was found to be 3.23 ± 0.06 and 3.01 ± 0.02 for anatase and rutile TiO_2, respectively based on data measured using the integrating sphere, as shown in Table 1. Similar E_g were calculated using data collected with the Praying Mantis diffuse reflectance accessory as well (Table 1), indicating consistent results can be acquired using both accessories. Both sets of calculated band gap energies are consistent with literature results as well[11,12] demonstrating both the integrating sphere and Praying Mantis can be reliably used for this application.

	Band gap energy (eV)	
	Integrating sphere	Praying mantis
Anatase TiO_2	3.23 ± 0.06	3.24 ± 0.05
Rutile TiO_2	3.01 ± 0.03	3.04 ± 0.02

Table 1. Calculated band gap energies for anatase and rutile TiO_2 determined from data collected using an integrating sphere (ISA-220) and the Praying Mantis diffuse reflectance accessory.

Conclusions

In this study, the Evolution UV-Visible spectrophotometers were used to acquire reflectance spectra for TiO_2 samples of varying crystal structure. Through use of the Tauc Plot analysis, the band gap energy was found to be approximately 3.0 eV and 3.2 eV for the rutile and anatase TiO_2 samples, respectively, matching literature values. The calculated band gap energy matched well for measurements collected with both the integrating sphere and Praying Mantis accessories, demonstrating reliability and consistency between the two methods. Though care should be taken when comparing samples measured using different baseline reflectance standards, the results included herein exhibit the ability to effectively analyze solid-state materials using the Evolution instruments and associated accessories.

References

1. Makula, P.; Pacia, M.; Macyk, W, How to Correctly Determine the Ban Gap Energy of Modified Semiconductor Photocatalysts Based on UV-Vis Spectra, *J. Phys. Chem. Lett.* **2018**, 9, 6814–6817.
2. Kapilashrami, M.; Zhang, Y., Liu, Y.-S.; Hagfeldt, A.; Guo, J., Probing the Optical Property and Electronic Structure of TiO_2 Nanomaterials for Renewable Energy Applications, *Chem. Rev.*, **2014**, 114, 9662-9707.
3. Zhao, Y.; Jia, X.; Waterhouse, G. I. N.; Wu, L.-Z.; Tung, C.-H.; O'Hare, D.; Zhang, T., Layred Double Hydroxide Nanostructured Photocatalysts for Renewable ENERGY Production, *Adv. Energ. Mater.*, **2016**, 6, 1501974.
4. Atkins, P., Shriver & Atkins' Inorganic Chemistry, Oxford University Press, 2010.
5. Weller, P. F.; An Analogy for Elementary Band Theory Concepts in Solids, *J. Chem. Ed.*, **1967**, 44, 391-393.
6. Kisch, H.; Macyk, W., Visible-Light Photocatalysis by Modified Titania, *ChemPhysChem*, **2002**, 3, 399-400.
7. Inamdar, S. N.; Ingole, P. P.; Haram, S. K., Determination of Band Structure Parameters and the Quasi-Particle Gap of CdSe Quantum Dots by Cyclic Voltammetry, *ChemPhysChem*, **2008**, 9, 2574-2579.
8. Jasieniak, J.; Califano, M.; Watkins, S. E., Size-Dependent Valence and Conduction Band-Edge Energies of Semiconductor Nanocrystals, *ACS Nano*, **2011**, 5, 5888-5902.
9. Coulter, J. B.; Birnie, D.P.; Assessing Tauc Plot Slope Quantification: ZnO Thin Films as a Model System, *Phys. Status Solidi B*, **2018**, 255, 1700393.
10. López, R.; Gómez, R., Band-Gap Energy Estimation from Diffuse Reflectance Measurements on Sol-Gel and Commercial TiO_2: A Comparative Study, *J. Sol-Gel Sci. Technol.*, **2012**, 61, 1-7.
11. Nosaka, Y.; Nosaka, A. Y., Reconsideration of Intrinsic Band Alignments within Anatase and Rutile TiO_2, *J. Phys. Chem. Lett.*, **2016**, 7, 431-434.
12. Miao, L.; Jin, P.; Kaneko, K.; Terai, A.; Nabatova-Gabain, N.; Tanemura, S, Preparation and Characterization of Polycrystalline Anatase and Rutile TiO_2 Thin Films by Rf Magnetron Sputtering, *App. Surf. Sci.*, **2003**, 212, 255-263.

Learn more at **thermofisher.com/evolution**